Turbulence Measurements in the Atmospheric Boundary Layer: A Comparison between Hot-wire and Sonic Anemometer Data.

André S. Monteiro, Juliana B. R. Loureiro and Atila P. Silva Freire
PEM/COPPE/UFRJ, C.P. 68503-21945-970, Rio de Janeiro, Brasil

Roberto Magnago, Osvaldo Moraes
Instituto de Física, Universidade Federal de Santa Maria, Santa Maria, Rio Grande do Sul

Abstract. *The purpose of this work is to compare the sonic anemometer response with hot-wire measurements at low level turbulence conditions that occur in highly stable conditions. Wind tunnel studies were conducted in order to assess the discrepancies in mean and turbulent data calculated from these two instrument responses. Power spectra of the hot-wire sensors were examined to evaluate the proper bandwidth response to produce reliable field measurements. The various problems encountered when using hot-wire in open atmosphere are addressed, This is a preliminary work in a joint effort between the Lab. Turbulence Mechanics(COPPE/UFRJ) and the Lab. of Micrometeorology of UFSM to probe the stable boundary layer aiming at improving further knowledge of the behavior of low level turbulence in atmospheric flows.*

Keywords: *Sonic anemometer, hot-wire anemometer, atmospheric boundary layer*

1. Introduction

Given the highly non-linear character of the governing equations of fluid motion and the immense difficulties in defining boundary conditions for atmospheric flows, it is inevitable to resort to some kind of experimental observation of real phenomena in order to develop a faithful modeling of the problem.

The earliest attempts to make quantitative measurements of the atmospheric turbulence can be traced back to G. I. Taylor. In 1917, he deduced some fundamental features of turbulent flows from observations of the gyrations of balloons and wind vanes. Among the assessed fundamental quantities were flow anisotropy and the eddy flux of momentum. However, one must keep in mind that early descriptions of the boundary layer had to rely entirely on data gathered from slow-response instruments that could yield just mean values.

Only in the late 60s fast-response instruments became available for field measurements. One of these instruments, and a very popular one, the sonic anemometer is, however, likely to have limited high frequency response when the turbulence scale is too small to be resolved by its path length. Therefore, their use near the ground, in calm winds and in very stable conditions is deeply in question. In these cases, a very small, fast response sensor is needed to resolve eddies responsible for heat and momentum transport. Consequently, hot-wire and hot-film anemometers are the only sensors currently available that meet the size and the high rate of signal acquisition that are normally required.

The question raised in the above paragraph is particularly relevant when we realize that the frequency response of a sonic anemometer does not exceed 350 Hz. The hot-wire anemometer, on the other hand, can withstand frequency responses of the order of 50 kHz. The low frequency response of the sonic anemometer frequently forces the experimenter to consider samples of up to 30 minutes. Under field conditions, this is, of course, a strong drawback.

The purpose of this work is to compare the sonic anemometer response with hot-wire measurements at low level turbulence conditions that occur in highly stable conditions. This will be made under controlled conditions in a wind tunnel. Thus, a wind tunnel study will be carried out to assess the discrepancies in both, mean and turbulent data, calculated from these two instrument responses. Power spectra of the hot-wire sensors were examined to evaluate the proper bandwidth response to produce reliable field measurements. The various problems encountered when using hot-wire in open atmosphere are also addressed. This is a preliminary work in a joint effort between the Lab. Turbulence Mechanics(COPPE/UFRJ) and the Lab. of Micrometeorology of UFSM to probe the stable boundary layer aiming at improving further knowledge of the behavior of low level turbulence in atmospheric flows.

2. Short literature review

Sozzi and Favaron (1996) studied the theoretical basis and presented a data-processing soft for both sonic- and thermo-anemometry. Arguing that the popularization of the sonic anemometer as a measuring technique is largely hampered by the few existing software packages, the authors strive at presenting methods for extraction the physically relevant parameters. Complementary, they showed how this information could be implemented to obtain real time information from sonic anemometers.

Moncrieff et al. (1997) developed an eddy covariance system to measure surface fluxes of momentum, sensible heat, water vapor and carbon dioxide. The system was based on a three-axis sonic anemometer, and on an IR gas analyzer. Sampling the turbulent data at 10 Hz, the system could be operated for the routine collection of surface data for extended

periods. The paper described a number of corrections that had to be applied to any standard eddy covariance system and described the system of transfer functions that defined their system.

The theory of sonic anemometer measurement was reviewed by Cuerva and Sanz-Andres (2000). The work solves the differential equations that describe the travel of ultrasound pulses in the general case of non-steady, non-uniform atmospheric flow field. To explain and evaluate the differences between the measured and the line-averaged turbulences, the concepts of instantaneous line-average and of traveling pulse-referenced average are introduced. The Kaimal (1968) maximum value limit that assesses the influence of the sonic measuring process on the estimated turbulent components was also reviewed. The paper analyzes three test cases. The mathematical model was then applied to situations of practical interest such as that of an anemometer located at a mast and that of the transfer function of a sensor in an atmospheric wind.

The interpretation of sonic anemometer data, the mathematical transformations necessary to obtain reliable results of mean and fluctuation velocities, and how they are influenced by instrument size, sampling frequency and measurement height were discussed by van Boxel et al. (2003). Turbulence spectra show the dominant frequencies in turbulent signals that contribute to the variance and the covariance of wind speed. For this reason, they must be correctly assessed so as to working out the measuring strategies of fast-response instruments such as the sonic anemometer. The friction velocity and the Reynolds stress (RS) are other important parameters to be determined. However, previous works have shown that RS sensitivity per degree of slope is very high, typically of the order of 9%. This uncertainty will result in an error of about 4% in the evaluation of the friction velocity. The work of Boxel et al. tackled all these issues.

An analysis of sonic anemometer observations in low wind speed conditions was presented by Anfossi et al. (2005). For very low wind speeds, that is for winds with low frequency horizontal oscillations, the definition of a preferential mean wind direction becomes very difficult. Analyzing the data from two sonic anemometers measuring campaigns, the authors showed that meandering exists irrespective of the meteorological conditions. The analysis also confirmed that wind meandering sets a lower bound for the horizontal wind component variances. In addition, the authors showed that the autocorrelation functions of the longitudinal wind components show an oscillating behavior with the presence of large negative lobes. Two different relations based on two different parameters were fitted to the data. Based on these relations, expressions for the mean square displacement of particles were advanced.

3. The hot-wire anemometer

Hot-wire anemometry (HWA) is based on the convective heat transfer process that takes place when a heated wire is exposed to a fluid flow (Perry (1982, Lomas (1986)). Because typical sensors are less than 5 νm in diameter and are made to withstand high temperatures, any change in fluid flow condition that affects the transfer of heat from the wire to the medium will be sensed immediately by a constant HWA system. HWA can then be used to measure the velocity and temperature of the flow, concentration and phase discrimination.

In general, one of the most important aspects of thermal anemometry is the accurate interpretation of the anemometer signal. The main purpose of any sensor calibration is to determine, as accurately as possible, the relationship between the anemometer output voltage and the physical property under consideration, in this case velocity or temperature. However, the direct output from all practical calibration procedures is raw calibration data, which will contain measurements uncertainties. An additional complication is that the true calibration curve of the probe is not known, and furthermore it depends on particular characteristics of each experiment.

Among the several possible methods that can be devised to characterize the velocity and temperature dependence of thermal anemometers signals, the linear correction method is the simplest. Through this procedure, the heat transfer from the probe is assumed to be proportional to a product of the temperature difference T_w - T_a and a function of the velocity, where T_w is the temperature of the heated wire and T_a is the ambient temperature. The output voltage, E, of a constant temperature hot-wire anemometer can hence be represented by:

$$\frac{E^2}{T_w - T_a} = (A + BU_n). \tag{1}$$

The most accurate way of establishing the velocity and temperature sensitivity of a constant temperature hot-wire probe, operated at a fixed hot resistance, R_w, is to measure the anemometer output voltage, E, as a function of the velocity, U, and fluid temperature, T_a. This type of calibration is often carried out by performing a velocity calibration at a number of different fluid velocities and temperatures.

Hot-wire probes are shown in Fig. 1 in position in a wind tunnel and from the Dantec catalog.

4. The sonic anemometer

Sonic anemometer are based on the Doppler effect. Thus, sonic anemometers measure wind velocity by evaluating the effects that the wind exerts the transition times of acoustic pulses traveling in opposite directions across a known path.

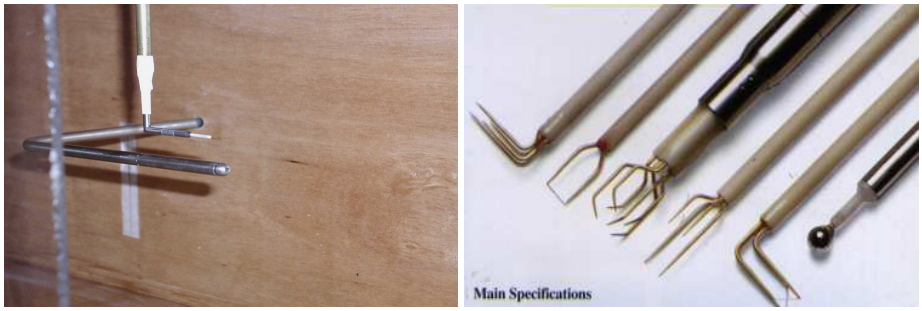

Figure 1. Hot-wire probes. (a) In the wind tunnel with a Pitot tube. (b) A selection from Dantec Measurement Tech.

Sonic anemometers can operate through two principles: pulsed or continuous regime.

Anemometers of the pulsed type measure the transit differences directly to evaluate the velocity component along a known path. On the other hand, anemometers of the continuous-wave type measure phase differences that can be converted to time differences.

The velocity component, U, along a path of length L, can be expressed as

$$U = \frac{c^2}{2L}(t_2 - t_1). \tag{2}$$

where c is the velocity of sound.

Provided U and L are known, U can then be evaluated directly from $(t_2 - t_1)$ through the above equation.

Probes that are required to give spatial discrimination of the velocity will require three defined paths.

The main limitation to the frequency response of a sonic anemometer results from the line averaging along the acoustic paths. Spatial separation between paths also introduces distortions at high-frequencies.

A sonic anemometer is shown in Fig. 2 fitted into the wind tunnel where the experiments were conducted.

Figure 2. Sonic anemometer in the wind tunnel.

5. The one-dimensional spectrum

The three-dimensional energy spectrum is one of the key concepts in turbulence theory (Hinze (1975), Tennekes and Lumley (1972)). However, in the laboratory or in nature, researchers find it much more convenient to measure the longitudinal spectrum. This, of course, sets the problem of relating the measured one-dimensional spectrum to the theoretical three-dimensional spectrum.

If a one dimensional flow has its movement captured by an anemometer, the velocity fluctuations may be decomposed into their harmonic components with respect to the angular frequency, ω. Then, by analyzing and averaging the signal, the resulting frequency spectrum, $E_{11}(\omega)$ must have the property

$$\left\langle u_1'^2 \right\rangle = \int_0^\infty E_{11}(\omega) d\omega. \tag{3}$$

To relate the frequency and wavenumber spectra, the common practice is to use the 'frozen convection' hypothesis of Taylor that considers the changes in u_1 with time at a fixed point to be due to the passage of a frozen pattern of turbulent motion.

This is equivalent to state

$$u(x,t) = u(x - \overline{u_1}t, 0), \tag{4}$$

or else,

$$\frac{\partial}{\partial t} = -\overline{u_1}\frac{\partial}{\partial x_1}. \tag{5}$$

The Taylor hypothesis is open to scrutiny even today, but it is at least a very good approximation and hence will be used extensively here.

Defining

$$E_{11}(k_1) = \overline{u_1}E_{11}(\omega), \quad k_1 = \omega/\overline{u_1}. \tag{6}$$

Then, it follows that

$$\int_0^\infty E_{11}(\omega)d\omega = \int_0^\infty \frac{E_{11}(k_1)d\omega}{\overline{u_1}} = \int_0^\infty E_{11}(k_1)dk_1 = \left\langle u_1'^2 \right\rangle. \tag{7}$$

An extension of the above equation to three dimensions is trivial, it suffices to integrate out the dependence of $E_{11}(k_1)$ on k_2 and k_3 to obtain

$$E(k) = \frac{k^3 d[k^{-1}dE_{11}(k)/dk]}{dk}. \tag{8}$$

6. Time domain analysis

The output signal of an anemometer is random by its very nature (Bruun (1995)). Therefore, a statistical description of its contents is in order. Next we will very briefly remind the reader some of the basic concepts in random data analysis and introduce the paper notation.

The autocorrelation function for the flow velocity is denoted by R_u, the autocorrelation coefficient function by ρ_u and the auto-spectral density function by S_u.

Consider a time-history velocity record, u. It can be split into a mean, $\overline{u}$ and a fluctuating component, u',through

$$u(t) = \overline{u} - u' \tag{9}$$

where the mean value is the average of all values, defined by

$$\overline{u} = lim_{T\to\infty}\frac{1}{T}\int_0^T u(t)\,dt. \tag{10}$$

In a digital data analysis, the continuous signal is replaced by a digital sample record. Taking T as the total sample time and N the corresponding number of samples, the sampling rate is given by $S_R = N/T = N\,F$.

Thus, the mean value of a finite sample record, $u(j)$, j = 1,2,..., N can be given by

$$\overline{u} = \frac{1}{N}\sum_{j=1}^{N} u(n). \tag{11}$$

The autocorrelation function shown the dependence of the data at one time in relation to the values at another time. An estimate of the autocorrelation function with a time delay $\tau = r/F$ can be written as

$$R_u(r/F) = \frac{1}{N-r}\sum_{j=1}^{N-r}\left[u(j) - \bar{u}\right]\left[u(j+r) - \bar{u}\right], \quad r = 0, 1, 2, \cdots, m. \tag{12}$$

where r is the lag number and m is the maximum lag number.

The autocorrelation coefficient function is defined by

$$\rho_u(r/F) = \frac{R_u(r/F)}{R_u(0)}. \tag{13}$$

The auto-spectral density function is defined in terms of a Fourier transform of the previously calculated correlation function

$$S_u(f) = \int_{-\infty}^{\infty} R_u(\tau) e^{-i2\pi f\tau}\, d\tau. \tag{14}$$

7. Small scales

Although the large eddies contribute to most of the transport of momentum and scalars, we know viscous dissipation of turbulence to be determined by the smallest of the eddies.

In this section, we will show how the smallest length scales in a turbulent flow can be found as a function of the auto-correlation function (Tennekes and Lumley (1972)).

Consider that small-scale motions have small time scales, which are statistically independent of the large scales. This argument leads to the conclusion that the rate of energy supply should equal the rate of dissipation. This is basis of Kolmogorov's universal equilibrium theory. This theory suggests that the microscales of length, time and velocity are given by

$$\eta = \left(\frac{\nu^3}{\varepsilon}\right)^{1/4}, \quad \varphi = \left(\frac{\nu}{\varepsilon}\right)^{1/2}, e \quad \upsilon = (\nu\varepsilon)^{1/4}. \tag{15}$$

The autocorrelation coefficient defines a further important microscale, Λ_u, which is defined by the curvature of ρ_u at the origin:

$$\left.\frac{d^2\rho_u(\zeta)}{d\zeta^2}\right|_{\zeta=0} = -\frac{2}{\Lambda_u^2} \tag{16}$$

The length scale Λ_u is called the Taylor time microscale; it is directly associated with the dissipation rate in a turbulent flow.

Expanding $\rho_u(\zeta)$ in a Taylor series around the origin, we can write for small values of ζ,

$$\rho_u(\zeta) \cong 1 - \frac{\zeta^2}{\Lambda_u^2}. \tag{17}$$

To correlate the Taylor time microscale with the longitudinal spectrum, we make

$$\overline{\left(\frac{du'}{dt}\right)^2} = 2\frac{\overline{u'u'}}{\Lambda_u^2}. \tag{18}$$

Then, applying Taylor hypothesis to the above equation,

$$\overline{\left(\frac{du'}{dx}\right)^2} = \frac{2}{\bar{u}^2}\frac{\overline{u'u'}}{\Lambda_u^2}. \tag{19}$$

The Taylor length microscale, χ_u, is given by

$$\overline{\left(\frac{du'}{dx}\right)^2} = \frac{\overline{u'u'}}{\chi_u^2}, \tag{20}$$

and the following relation holds

$$\chi_u = \frac{\bar{u}}{\sqrt{2}}\Lambda_u \tag{21}$$

Finally, considering the turbulence isotropic, the dissipation rate, ϵ, can be evaluated from

$$\epsilon = 15\nu\frac{\overline{u'\,u'}}{\chi_u^2}. \tag{22}$$

8. Experimental Facilities

In this section, will be described the wind tunnel facilities at Laboratorio de Mecânica da Turbulência (COPPE/UFRJ). A complete description of the hot-wire and of the sonic anemometer will also be reported.

8.1 Wind Tunnel

The wind tunnel to be used in this work is a low-turbulence wind tunnel with turbulence intensity levels of the order of 0.2% with open circuit. This wind tunnel can be set to run at velocities that can reach 13 m/s; the test section is 4 m long, the cross section area is 0.30 x 0.30 m. This tunnel was adapted for the calibration of the cold-wire with the inclusion of a new heating section. The heating section was built with four electrical resistances in series, each one of them consisting of strings distributed transversally to the flow.

The wind tunnel is fitted with honeycombs and screens to control the turbulence levels and to guarantee a uniform flow. The computer-controlled traverse gear system is two-dimensional and capable to position sensors with an accuracy of 0.02 mm. The details of the wind tunnel are shown in Fig. 3.

Figure 3. Picture of wind tunnel.

8.2 Instrumentation

In all experiments, simultaneous measurements of stream-wise velocity and fluctuating temperature were made through sonic and thermal anemometry.

The sonic anemometer results were obtained with a one-dimensional anemometer manufactured by Campbel Inc. The data acquision software was also furnished by this company, model PC208W DATALOGGER.

The measurements took into account any changes in room temperature. To perform the measurements a temperature-compensated Dantec probe, model 55P76, was used. This probe consists of two sensor elements: a hot-wire and a resistance-wire, usually called cold-wire, situated 2 mm below and 5 mm downstream of the former. Both sensors are Pt-plated tungsten wires, 5 μm in diameter, 3 mm in overall length, and sensitive wire length of 1.25 mm. They are copper and gold plated at the ends to approximately 30 μm. They were connected respectively to a constant temperature bridge, Dantec 55M10 and to a constant current bridge, Dantec 56C20.

Reference measurements for velocity was obtained from a Pitot tube connected to an inclined manometer; temperature reference data was obtained from previously calibrated micro-thermocouples.

In getting the data, 10,000 samples were considered. The reference mean temperature profiles were obtained through a chromel-constantan micro-thermocouple mounted on the same traverse gear system used for the hotwire probe. An uncertainty analysis of the data was performed according to the procedure described in Kline (1985). Typically the

uncertainty associated with the velocity and temperature measurements were: U = 0.0391 m/s precision, 0 bias (P=0.95); T = 0.2 ^oC precision, 0 bias (P=0.99).

To obtain accurate measurements, the mean and fluctuating components of the analogical signal given by the anemometer were treated separately. Two output channels of the anemometer were used. The mean velocity profiles were calculated directly from the untreated signal of channel one. The signal given by channel two was 1 Hz high-pass filtered leaving, therefore, only the fluctuating velocity. The latter signal was then amplified with a gain controlled between 1 and 500 and shifted by an offset so as to adjust the amplitude of the signal to the range of the A/N converter.

9. Results

All mean velocity and temperature data are to be referred to the data obtained with the Pitot tube and the thermocouples.

Setting the Pitot as a standard for the velocity measurements was crucial. That is because the data furnished by the sonic anemometer provides a mean velocity that is off-set from the real flow velocity. This shifted value then needs to be corrected against some standard.

Since in the wind tunnel the flow direction is known, the sonic anemometer had to placed with its path aligned with the flow direction. The same procedure was adopted for the hot-wire anemometer and the Pitot tube, they were all aligned to the flow.

After the alignment process, a comparison was made between measurements obtained through the hot-wire and sonic anemometers. Data for the sonic anemometer was obtained with a frequency of 10 Hz, whereas the data for the hot-wire was obtained with a frequency of 10 kHz. The measurements had a 70 second duration. Thus, typical hot-wire and sonic ensembles had 700,000 and 700 samples respectively.

At first, a calibration was made for each of the two techniques (hot-wire and the sonic anemometers) by controlling the velocity of the tunnel. These calibrations were tested against the velocity data obtained through a Pitot Tube. In the case of the hot-wire anemometer, the constants A and B of the calibration curve were obtained by a linear regression of the points $[E^2/(T_w - T_a); U^{0.45}]$. In the case of the sonic anemometer, the differences between the measured velocities and the Pitot tube readings was evaluated for several values. The average offset was then used to correct the sonic anemometer readings (Table 1).

$U_{pitot}(m/s)$	$E_{hwa}(Volts)$	$U_{hwa}(m/s)$	$U_{Sonic}(m/s)$	$U_{pitot} - U_{Sonic}$	$U_{sonic}corrected(m/s)$
0.0150	3.0862	0.0162	-0.4657	0.4807	-0.0560
0.9506	3.4484	0.9889	0.6255	0.3251	1.0352
1.3440	3.4960	1.2663	0.6258	0.5182	1.2355
1.6465	3.5409	1.5670	1.0706	0.5759	1.4803
1.9013	3.5836	1.8902	1.4421	0.4592	1.8518
2.1257	3.6209	2.2036	1.8107	0.3150	2.2204
2.5151	3.6575	2.5405	2.1239	0.3912	2.5336
2.8519	3.6904	2.8693	2.4811	0.3708	2.8908
3.1529	3.7210	3.1978	2.9477	0.2052	3.3574
3.5570	3.7496	3.5254	3.1017	0.4553	3.5114
			mean	0.4097	
			off-set	0.4097	

Table 1. Table 1. Calibration procedure for hot-wire and sonic anemometers.

A comparison between the mean velocity values and the velocity fluctuations obtained through the hot-wire and the sonic anemometers was made (Table 2). It was observed that for the lower velocity values, the error in the fluctuation measurements exceeded 100%. This can have a great influence in the results, due to the low speed conditions that commonly occur in the atmospheric boundary layer.

A further data set was used to analyze the autocorrelation function values for the hot-wire and the sonic anemometers. The hot-wire data consisted of 30000 points of instantaneous velocity values, collected at 1000 Hz for 30 seconds. The sonic data also consisted of 30000 points, which were collected at the usual sonic anemometer frequency of 10Hz, for a duration of 50 minutes.

The autocorrelation function is defined for u as $R_u(\zeta) = \overline{u'(\theta)u'(\theta + \zeta)}$, where θ is the instantaneous time and ζ is the delay time. Considering that $u(\theta) = \bar{u} + u'(\theta) \Rightarrow u'(\theta) = u(\theta) - \bar{u}$, the discrete values of R_u were obtained by the equation [Brunn (1995), pp. 430]:

$U_{hwa}(m/s)$	$u'_{hwa}(Volts)$	$IT_{hwa}(\%)$	$U_{Sonic}(m/s)$	$u'_{Sonic}(m/s)$	$IT_{sonic}(\%)$	$ErroU(\%)$	$ErroIT(\%)$
3.5254	0.0180	0.5117	3.5176	0.0297	0.8440	0.2225	64.9353
3.0481	0.0169	0.5554	3.0302	0.0280	0.9234	0.5221	66.2529
2.0556	0.0130	0.6358	2.0539	0.0253	1.2328	0.0837	93.8940
1.1216	0.0081	0.6358	1.1813	0.0165	1.3981	5.3188	119.8955
0.8528	0.0059	0.7028	0.9139	0.0172	1.8813	7.1703	169.6884

Table 2. Table 2. Comparison in the values of the mean velocity and the velocity fluctuations.

$$R_u(r/F) = \frac{1}{N-r}\sum_{j=1}^{N-r}\left[u(j)-\bar{u}\right]\left[u(j+r)-\bar{u}\right], \tag{23}$$

where r is known as the delay number. The number of discrete points obtained for the autocorrelation function is equal to $m+1$, because $r = 0, 1, 2, \cdots, m-2, m-1, m$, where m is maximum delay time.

The definition and the method of acquisition of the discrete values for the autocorrelation function [Brunn (1995), pp. 429] is shown below:

$$\rho_u(\zeta) = \frac{R_u(\zeta)}{R_u(0)} \Rightarrow \rho_u(r/F) = \frac{R_u(r/F)}{R_u(0)} \tag{24}$$

Comparisons were made for two mean velocities: $1.08\ m/s$ and $3.17\ m/s$.

In the autocorrelation function results that were obtained for $1.08\ m/s$, it was observed that the flow begins to be dominated by a low frequency oscillation. This fact is not observed for the velocity of $3.17\ m/s$, indicating that this phenomenon only occurs at low velocities.

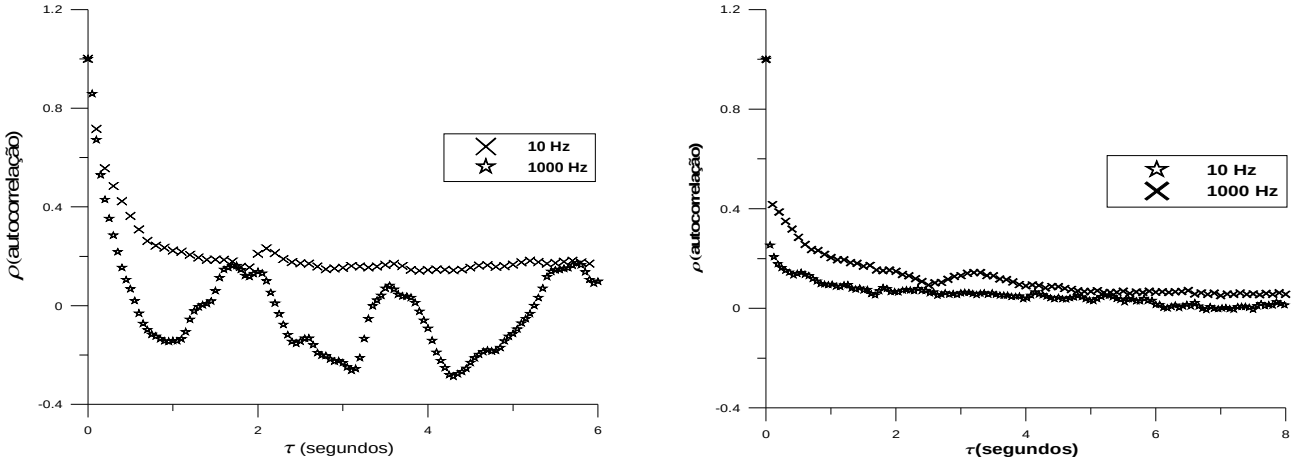

Figure 4. Autocorrelation function for $1.08\ m/s$ and $3.17\ m/s$.

The low frequency oscillations (meanders) which begin to dominate the flow overcome both the transport and the small-scale diffusion. As mentioned above, low speed conditions are common across space and time in the ABL.

Another feature observed by comparison of the two autocorrelation functions found for the hot wire and the sonic anemometers is the fact that the points collected by the sonic anemometer still take a longer time to reach an uncorrelated state than the points collected by the hot wire anemometer. This fact was observed to occur for comparisons made for the two velocities: $1.08\ m/s$ and $3.17\ m/s$. Furthermore, for the lower speed the correlation for the sonic anemometer data requires a longer time to set in.

The Taylor micro-scale and the dissipation per mass unit evaluated from both anemometers is shown below in Table 3.

10. Final remarks

The present work has carried out a preliminary investigation on the relative performances of hot-wire and sonic anemometers. At the present stage, the results were not encouraging. Given the controlled conditions found in a wind

Table 3. Taylor length micro-scale and the dissipation rate per mass unit according to both anemometers at $\overline{U}$ = 3.17 m/s and u'= 0.02 m/s.

Anemometer	Taylor length micro-scale (mm)	Dissipation rate per mass unit (m^2/s^3)
Hot-wire	1.87	0.025813
sonic	175.05	0.000003

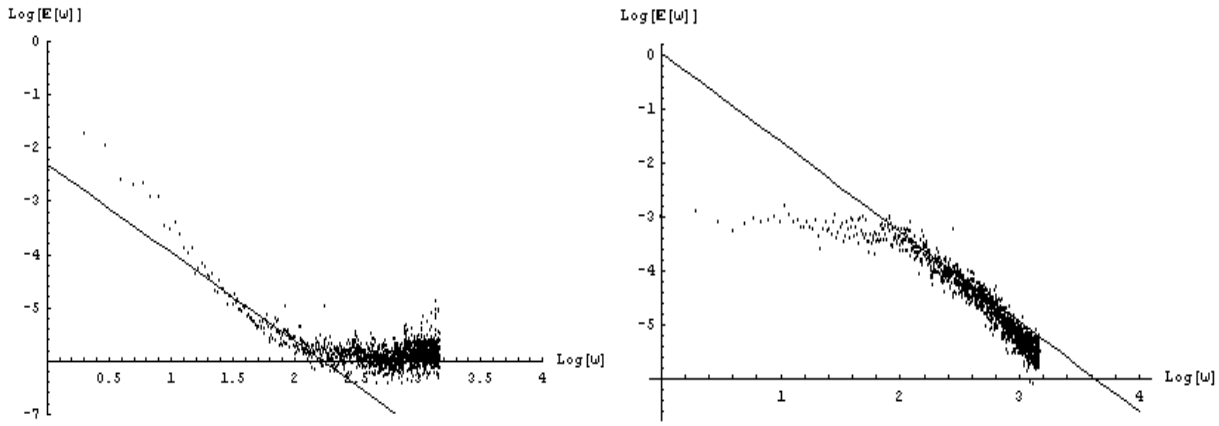

Figure 5. Velocity Spectra through the hot-wire and sonic anemometers $\overline{U}$ = 3.17 m/s.

tunnel, the results presented by both anemometers should be much better. As it stands, the results for the auto-correlation function and for the spectrum did not match very well. The real consequence is that turbulent energy levels and the integral scales of turbulence will not be faithfully assessed.

Currently, new measurements are being undertaken so as to cross check all the present findings. This will be reported elsewhere.

Acknowledgements. APSF is grateful to the Brazilian National Research Council (CNPq) for the award of a research fellowship (Grant No 304919/2003-9). The work was financially supported by CNPq through Grant No 472215/2003-5 and by the Rio de Janeiro Research Foundation (FAPERJ) through Grants E-26/171.198/2003 and E-26/152.368/2002. ASM benefited from a MSc Scholarship from the Brazilian Ministry of Education (CAPES/MEC).

11. References

Anfossi, D., Oettl, D., Degrazia, G. and Goulart, A.; 2005, "Analysis of sonic anemometer observations in low speed conditions", Boundary Layer Meteorology, 114, 179-203.

Bruun, H. H.; "Hot-Wire Anemometry, Principles and Signal Analysis", Oxford University Press, 1995.

Cuerva, A. and Sanz-Andres, A.; 2000, "On sonic nemometer measurement theory", Journal of Wind Engineering and Ind. Applications, 25-55.

Lomas, C. G.; 1986, "Fundamentals of Hot-wire Anemometry", Cambridge University Press, Cambridge.

Hinze, J. O., 1975, "Turbulence - Second edition". McGraw-Hill, Inc.

Moncrieff, J. B.; 1997, "A system to measure surface fluxes of momentum, sensible heat, water vapour and carbon dioxide", J. Hydrology, 188-189, 589-611.

Perry, A.E.; 1982, "Hot-wire Anemometry", Oxford University Press.

Sozzi, R. and Favaron, 1996, M., Sonic anemometer and thermometry: theoretical basis and data-processing software, Environmental Software, 11, 4 259-270.

Tennekes, H. And Lumley, J. L., 1972, A first course in turbulence, MIT Press.

Van Boxel, J. H., Sterk, G. and Arens, S. M., 2004; "Sonic anemometer in aeolian sediment transport researcht't', Geomorphology, 59, 131-147.